JACS
JOURNAL OF THE AMERICAN CHEMICAL SOCIETY

Communication

pubs.acs.org/JACS

Aqueous-Phase Reactions on Hollow Silica-Encapsulated Semiconductor Nanoheterostructures

Jie Lian,[†,‡] Yang Xu,[†] Ming Lin,[‡] and Yinthai Chan*[,†,‡]

[†]Department of Chemistry, National University of Singapore, 3 Science Drive 3, Singapore 117543

[‡]Institute of Materials Research and Engineering, A*STAR, 3 Research Link, Singapore 117602

Supporting Information

ABSTRACT: We introduce a facile and robust methodology for the aggregation-free aqueous-phase synthesis of hierarchically complex metal−semiconductor heterostructures. By encapsulating semiconductor nanostructures within a porous SiO_2 shell with a hollow interior, we can isolate each individual particle while allowing it access to metal precursors for subsequent metal growth. We illustrate this by Pt deposition on CdSe-seeded CdS tetrapods, which we found to be facilitated via the surprising formation of a thin interfacial layer of PtS coated onto the original CdS surface. We took advantage of this unique architecture to perform cation exchange reactions with Ag^+ and Pd^{2+}, thus demonstrating the feasibility of achieving such transformations in complex metal−semiconductor nanoparticle systems.

The development of the composition and morphological control of multicomponent hybrid nanoparticles has in recent times been an area of intense research, fueled by their possible relevance in applications of growing importance such as photocatalysis,[1] biological imaging,[2] and photovoltaics.[3] Among the plethora of colloidal heterostructured nanoparticles reported, anisotropic hybrid metal−semiconductor nanostructures are particularly interesting because of their potential capacity for directed or end-to-end assembly,[4] enhanced electrical conductivity,[5] and improved charge separation at the metal−semiconductor interface.[1] To date, a wide variety of metal nanoparticles such as Au, Co, and alloyed Pd−Au[6] have successfully been deposited either at tip-specific regions or throughout the surface of cadmium chalcogenide nanorods and branched structures. The deposition of Pt on CdS is particularly interesting in view of their potential utility in the photocatalytic reduction of water into hydrogen,[7] but the growth of Pt on colloidal cadmium chalcogenide nanostructures requires specialized Pt precursors in an organic solvent at either high temperature[8] or under UV illumination.[9] Moreover, the surface coverage of Pt on the semiconductor is typically low, which is not optimal for photocatalysis. On the other hand, aqueous synthetic routes employing common Pt precursors can yield a much higher Pt surface coverage, although the resulting particles are highly prone to agglomeration, requiring stringent pH-controlled conditions to avoid fusion of the particles into large structures.[10]

Herein we propose an alternative approach to the conventional metal deposition process in which the host semiconductor is first isolated within a porous SiO_2 nanostructure with a hollow interior that permits exposure to the metal precursors and allows for their subsequent heterogeneous nucleation and growth on the semiconductor surface. We chose semiconductor tetrapods because such structures typically provide extremely large absorption cross sections on a per particle basis in comparison with their spherical and rodlike counterparts,[11] making them very well suited for supporting photoinduced reactions. A schematic illustration of the fabrication of such hollow SiO_2 tetrapod composites is shown in Figure 1A. The synthesis of monodisperse CdSe-seeded CdS tetrapods proceeded according to a previously reported method[12] with slight modifications [see the Supporting Information (SI)]. Encapsulation with a shell of silica was then carried out using a previously reported reverse microemulsion approach in which the as-synthesized hydrophobic semiconductor tetrapods in cyclohexane were exposed to silica precursors in the presence of the surfactant Igepal CO-520 and water,[13] resulting in silica-coated structures (Figure 1B). This allowed for the tetrapods to be easily dispersed and colloidally stable in aqueous solutions.

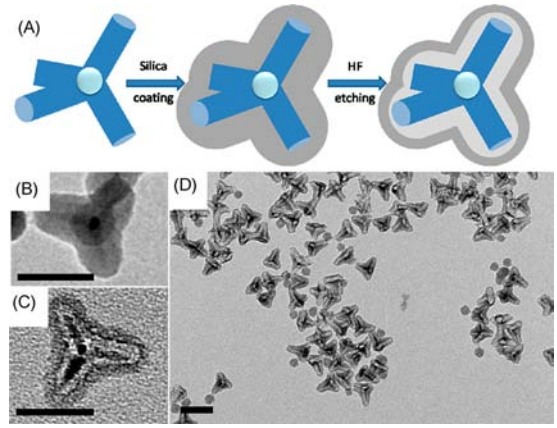

Figure 1. (A) Schematic illustration of the formation of SiO_2-encapsulated semiconductor tetrapod structures with a hollow interior. (B) Magnified TEM image of a typical silica-coated CdSe-seeded CdS tetrapod. (C, D) Images of silica-coated tetrapods with a hollow silica interior at high and low magnification, respectively. Scale bars = 50 nm.

Received: February 23, 2012
Published: May 10, 2012

   dx.doi.org/10.1021/ja301805u | J. Am. Chem. Soc. 2012, 134, 8754−8757

It was recently reported that the growth of silica around nanoparticles via a Stöber-type process can result in a structurally inhomogeneous shell in which the innermost layer is "soft", with a porous structure that possesses a lower degree of Si−O cross-linking, and an outermost layer that is "hard" and highly cross-linked.[14] We hypothesized that our SiO_2 shells possessed a similar structural inhomogeneity, which we subsequently exploited to remove the innermost layer of silica selectively via exposure to dilute HF. By optimizing the etching parameters such as reaction time and acid concentration, we reproducibly obtained very monodisperse semiconductor tetrapods encased within the hollow interior of a structured silica matrix (Figure 1C,D). The porosity of the "hard" layer, which facilitated acid diffusion into the "soft" SiO_2 layer and subsequent diffusion of the etched contents out, should in principle also allow for a large variety of small molecules or ions to access the semiconductor surface.

To derive various morphologies of Pt deposited on CdSe-seeded CdS tetrapods, different amounts of H_2PtCl_6 precursor were dissolved in water and mixed vigorously with the hollow silica-encapsulated tetrapods for 2 h at 60 °C. While relatively low concentrations of H_2PtCl_6 did not result in any observable Pt deposition, intermediate concentrations yielded very small particles with diameters of 0.8−1.2 nm. Further increasing the amount of added Pt precursor led to the growth of larger Pt nanoparticles (Figure 2A). It is evident that the Pt particles are

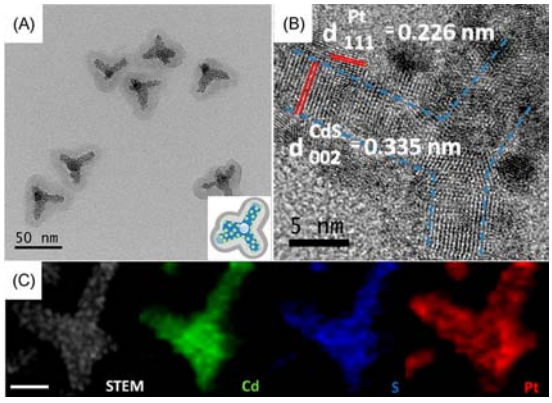

Figure 2. (A, B) TEM images of CdSe-seeded CdS tetrapods decorated with Pt particles at low and high magnification, respectively. Discernible lattice constants of 0.226 and 0.335 nm are attributed to the Pt {111} and CdS {002} planes, respectively. (C) Chemical mapping of elements Cd, S, and Pt for Pt-decorated CdSe-seeded CdS tetrapods: HAADF-STEM images showing (left to right) Cd (green), S (blue), and Pt (red). Scale bar = 20 nm.

located in fairly high density along the tetrapod arms, in contrast with previously reported decoration of tetrapod tips with Au particles[6] and in agreement with Pt deposition on CdSe nanorods in the aqueous phase.[10] Although the reduction of the Pt precursor in the absence of light, oxygen, or a reducing agent was previously seen in Pt-deposited CdSe nanorods and ascribed to a redox process between Pt^{4+} and Se^{2-},[10] the reduction of the Pt precursor in our system is unlikely to have proceeded via the oxidation of S^{2-}, as we did not observe any discernible decrease in the dimensions of the CdS tetrapod arms. On the other hand, a control experiment in which the Pt precursor was heated in water showed the presence of irregularly shaped Pt clusters (see the SI), suggesting that water is the reductant under the reaction conditions employed, as observed previously by Viswanath et al.[15] The thin silica shell permitted analysis via high-resolution transmission electron microscopy (HRTEM) (Figure 2B), which revealed the presence of lattice fringes of both CdS and Pt, the latter of which appeared to be randomly oriented with respect to the axis of the CdS tetrapod arm. Further confirmation of the composition of the tetrapod heterostructures was carried out via elemental mapping of Cd, S, and Pt on individual tetrapods, as may be inferred from the composite image shown in Figure 2C. High-angle annular dark-field scanning TEM (HAADF-STEM) analysis of the silica-encapsulated, Pt-decorated CdSe/CdS tetrapods yielded a clear contrast between the semiconductor and metal domains, allowing the diameters of the Pt nanoparticles formed (typically 1.5−2.5 nm) to be reliably determined (see the SI).

To emphasize the importance of the hollow encapsulation of anisotropic semiconductor nanostructures undergoing metal deposition processes in aqueous media, a number of control experiments entailing bare semiconductor tetrapods were conducted as follows. As-synthesized CdSe-seeded CdS tetrapods were first rendered water-dispersible by surface ligand exchange with 11-mercaptoundecanoic acid (MUA)[16] and then allowed to undergo the same reaction conditions as described above for the silica-encapsulated tetrapods. This resulted in serious aggregation, and only a very small quantity of smaller clusters of tetrapods could be recovered and characterized via TEM, though it may be seen that Pt nucleation and growth did occur on the aggregated particles (see the SI). A second control experiment was performed in which silica-encapsulated semiconductor tetrapods without a hollow interior were used, with all of the other reaction conditions being equivalent to those for their hollow counterparts. Despite the use of a fairly large range of Pt concentrations, no sign of any Pt deposition was observed (see the SI). This is likely due to the intimate contact between CdS and the silica shell, which would inhibit nucleation and growth of Pt particles on the semiconductor surface, thus justifying the need for encapsulation of the semiconductor nanostructures within a hollow interior.

An intriguing observation was made in which hollow silica-encapsulated tetrapods exposed to relatively low concentrations of Pt precursors showed no signs of Pt nucleation and growth yet gave an appreciable Pt signal under energy-dispersive X-ray spectroscopy (EDX) characterization. The persistence of the Pt signal even under very rigorous washing conditions, which excluded the remote possibility of Pt precursor contamination in the sample background, prompted further investigation. Exposure to a mixture of dilute HF and HCl resulted in the total removal of the SiO_2 shell and the Cd chalcogenide moieties, leaving behind an extremely thin (∼ 1 nm) hollow layer that preserved the shape characteristics of the original tetrapod structures (Figure 3A). Treating CdSe-seeded CdS tetrapods bearing large Pt particles with the acid mixture resulted in the preservation of the Pt particles atop the thin hollow tetrapod structure (Figure 3B). A more definitive image of the thin hollow layer with good image contrast was afforded by HAADF-STEM (Figure 3C), and an analysis of the dimensions of the tetrapod structures suggested negligible differences with the original Cd-based tetrapods. While EDX measurements (Figure 3D) surprisingly showed the absence of Cd and the presence of Pt and S in an atomic ratio of 1:1, a line scan across the arm of the tetrapod structure revealed a composition profile consistent with a hollow interior (Figure

dx.doi.org/10.1021/ja301805u | J. Am. Chem. Soc. 2012, 134, 8754−8757

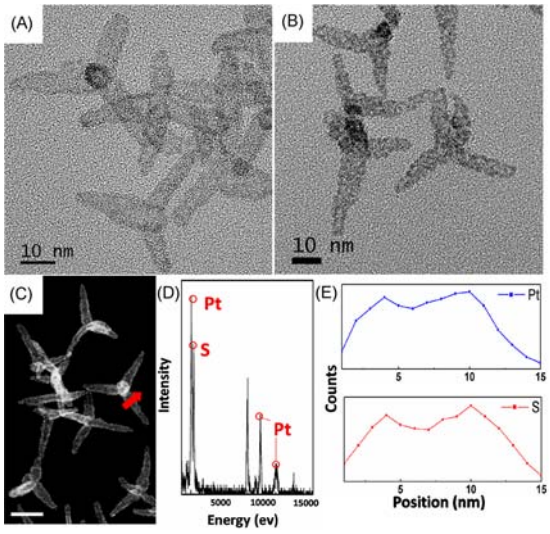

Figure 3. (A, B) TEM images of hollow PtS tetrapods and hollow PtS tetrapods with deposited Pt particles, respectively. (C) HAADF-STEM image of representative hollow PtS tetrapods. Scale bar = 20 nm. (D) EDX spectrum of Pt particles deposited PtS tetrapods, showing only Pt and S signals. The quantified results show Pt and S percentages of 51.02 and 49.24 atom %, respectively. (E) Corresponding EDX line scan across one arm of a hollow PtS tetrapod using scan steps of 0.2 nm.

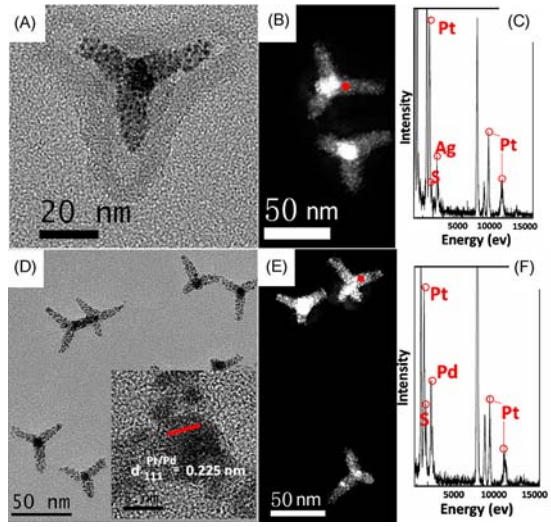

Figure 4. (A) TEM image of a Pt-nanoparticle-decorated Ag_2S tetrapod. (B, C) Corresponding (B) HAADF-STEM and (C) EDX data for (A). The quantified percentages of Ag, S, and Pt are 35.23, 19.08, and 45.69 atom %, respectively. (D) TEM image of Pt-nanoparticle-decorated PdS tetrapods without the SiO_2 shell. The inset is an HRTEM image showing the lattice fringes of the Pt–Pd alloy {111} plane. (E, F) Corresponding (E) HAADF-STEM and (F) EDX data for (D), yielding Pd, S, and Pt percentages of 29.77, 22.01, and 48.22 atom %, respectively.

3E). On the basis of our experimental observations and the unlikelihood of pure Pt growth on CdS (which has a lattice mismatch of ~32.4%, as opposed to ~3.6% for PtS on CdS), we conclude that the composition of the thin interfacial layer is most likely that of PtS. The absence of clear lattice fringes in HRTEM and the lack of distinct peaks in X-ray diffraction measurements suggest that this PtS layer is likely to be amorphous, which is not unexpected given its formation via partial cation exchange at a relatively low temperature of ~60 °C. Further confirmation of the assignment of PtS was provided by X-ray photoelectron spectroscopy, which showed a strong PtS peak and a smaller PtO peak at 72.8 and 74.1 eV, respectively (see the SI). Efforts to elucidate the physicochemical properties of such ultrathin semiconductor nanostructures are presently ongoing.

Although it has been shown that complex-shaped semiconductor nanoparticles can undergo cation exchange while retaining the structural characteristics of the anionic sublattice,[17] ion exchange processes in colloidal hybrid metal–semiconductor nanostructures have scarcely been explored. We surmised that the thin amorphous interfacial layer of PtS supporting the growth of nanoparticles of Pt could facilitate cation exchange of the underlying CdS structure while preserving the architectural framework of the Pt-decorated surface, thus exemplifying a novel strategy for the fabrication of hierarchically complex metal–-semiconductor nanoparticles. To validate this supposition, silica-coated, Pt-functionalized CdSe-seeded CdS tetrapods were exposed to an aqueous solution of Ag^+ and allowed to react for ~1 h under ambient conditions. Characterization via TEM (Figure 4A and the SI) indicated that the resulting structures bore the shape of the initial tetrapods and were decorated with particles of a much darker contrast. The compositional profile of the particles was characterized via STEM and EDX, which showed only the presence of Ag, S, and Pt (Figure 4B,C). The prominent absence of Cd suggested that the obtained structures consisted of Ag_2S tetrapods and Pt nanoparticles separated by a thin interfacial layer of PtS, analogous to the Pt-decorated CdSe-seeded CdS tetrapods with a PtS layer. Quantification of the EDX signals revealed an Ag/S ratio of approximately 2:1, consistent with a Pt-decorated CdSe-seeded CdS tetrapod undergoing full cation exchange with Ag^+ without loss of the Pt particles.

To determine whether Pt particles may be directly grown on cation-exchanged Ag_2S tetrapods, control experiments were performed in which MUA-capped CdSe-seeded CdS tetrapods dispersed in the aqueous phase were first exposed to Ag^+, after which the Pt precursor H_2PtCl_6 was added. Amidst particle aggregation, no sign of Pt deposition was observed via TEM, although careful EDX measurements detected a very weak presence of Pt that was likely originated from extremely small clusters of Pt on top of the fully cation-exchanged Ag_2S surface. The same reaction conditions were carried out with SiO_2-encapsulated CdSe/CdS tetrapods in which cation exchange with Ag^+ took place before exposure to the Pt precursor. Despite the relatively high concentrations of Pt precursor explored, no evidence of Pt deposition on the Ag_2S tetrapod arms was observed. These observations highlight the importance of our strategy in fabricating geometrically complex Pt-decorated semiconductor nanostructures under mild reaction conditions, where the affinity between Pt and the semiconductor is low and direct growth of large Pt nanoparticles onto the semiconductor surface is difficult. However, it should be mentioned that the heterogeneous nucleation of Pt on spherical Ag_2S nanoparticles was previously achieved under refluxing conditions and in the presence of a reducing agent.[18] In the case of the Pt-decorated tetrapods with Ag_2S arms, preservation of the Pt nanoparticle network was likely also facilitated by the fact that the Cd^{2+} undergoes exchange with Ag^+, whereas Pt^{2+} does not (see the SI). Indeed, for Au-decorated CdSe-seeded CdS tetrapods, in which an interfacial

dx.doi.org/10.1021/ja301805u | J. Am. Chem. Soc. 2012, 134, 8754–8757

layer of gold sulfide is not formed because the Au ions do not undergo cation exchange with Cd^{2+} in CdS,[6] exposure to Ag^+ resulted in the partial removal of Au particles. It may be speculated that this occurs where the Cd^{2+} in the vicinity of the Au particles were replaced with Ag^+ (see the SI).

In view of the unique ability of the thin amorphous PtS layer to facilitate cation transfer between the solvent bath and the underlying CdS nanostructure while supporting a dense distribution of Pt nanoparticles, it may be envisaged that a multitude of anisotropic, hierarchically complex, Pt-decorated semiconductor nanocomposites may be synthesized. As an example, we selected PdS as a choice material because of its utility as a catalyst[19] and its potential synergistic relationship with the well-known catalytic properties of Pt. Thus, Pt-decorated CdSe-seeded CdS tetrapods with an interfacial layer of PtS were allowed to undergo cation exchange with Pd^{2+}. Despite a large fractional volume change ($|\Delta V/V| \approx 0.315$ based on bulk lattice parameters), which can result in drastic shape change,[20] TEM characterization of the Pt-decorated PdS tetrapod structures (Figure S6A in the SI) suggested that the cation exchange process preserved the structural integrity of the original Pt-deposited semiconductor tetrapods. This is also apparent in Figure 4D, which shows that the Pt nanoparticles were still present atop the tetrapod-shaped heterostructures even after the SiO_2 shell was removed. Further investigation via HAADF-STEM and EDX (Figure 4E,F) showed the presence of Pt, S, and Pd only, thus corroborating our supposition that full cation exchange between Cd^{2+} and Pd^{2+} had occurred. The measured Pd/S ratio in the structure was approximately 1.3:1, consistent with an oxidation state of Pd^{2+} and an overall PdS composition. We conjectured that the additional Pd signal might be due to the deposition of Pd on the Pt particles in some of the tetrapods, forming an alloy. The inset in Figure 4D shows an example of such a structure in which some of the nanoparticle sizes increased to 3−4 nm after exposure to Pd and exhibited lattice spacings commensurate with a Pt−Pd alloy.

In summary, we have reported a facile and robust methodology for the aggregation-free aqueous-phase synthesis of hierarchically complex metal−semiconductor heterostructures. By encapsulation with a SiO_2 shell having a hollow interior, an intricately shaped semiconductor nanoparticle can be isolated and allowed to undergo metal deposition and cation exchange reactions without problems of irreversible particle agglomeration. We have demonstrated the utility of this technique using Pt deposition on CdSe-seeded CdS tetrapods, which we found to be facilitated via the surprising formation of a thin interfacial layer of PtS coated onto the CdS surface. We took advantage of this unique architecture and high colloidal stability of the Pt-decorated semiconductor particles to make them undergo subsequent cation exchange reactions with Ag^+ and Pd^{2+}, yielding Pt-nanoparticle-decorated Ag_2S and PdS tetrapods, respectively. To the best of our knowledge, the synthesis of these nanocomposites is unprecedented, and their potential utility as catalysts is currently being investigated. More importantly, the circumvention of particle aggregation using hollow silica shells allowed for aqueous-phase metal deposition and cation exchange processes to be used in a sequential fashion, thus providing a robust and facile synthetic route to anisotropic metal−semiconductor nanostructures.

■ ASSOCIATED CONTENT

Supporting Information

Synthesis details, UV−vis absorption spectra, and TEM characterizations. This material is available free of charge via the Internet at http://pubs.acs.org.

■ AUTHOR INFORMATION

Corresponding Author

chmchany@nus.edu.sg

Notes

The authors declare no competing financial interest.

■ ACKNOWLEDGMENTS

This work was supported by DSTA (WBS R143-000-423-422) and TSRP-A*STAR (WBS R143-000-435-305).

■ REFERENCES

(1) Costi, R.; Saunders, A. E.; Salant, A.; Banin, U. *Nano Lett.* **2008**, *8*, 637.

(2) Choi, J. S.; Jun, Y. W.; Yeon, S. I.; Kim, H. C.; Shin, J. S.; Cheon, J. *J. Am. Chem. Soc.* **2006**, *128*, 15982.

(3) Yoshino, K.; Ikari, T.; Shirakata, S.; Miyake, H.; Hiramatsu, K. *Appl. Phys. Lett.* **2001**, *78*, 742.

(4) (a) Zhao, N.; Liu, K.; Greener, J.; Nie, Z.; Kumacheva, E. *Nano Lett.* **2009**, *9*, 3077. (b) Salant, A.; Amitay-Sadovsky, E.; Banin, U. *J. Am. Chem. Soc.* **2006**, *128*, 10006. (c) Figuerola, A.; Franchini, I. R.; Fiore, A.; Mastria, R.; Falqui, A.; Bertoni, G.; Bals, S.; Tendeloo, G. V.; Kudera, S.; Cingolani, R.; Manna, L. *Adv. Mater.* **2009**, *21*, 550.

(5) Sheldon, M. T.; Trudeau, P. E.; Mokari, T.; Wang, L. W.; Alivisatos, A. P. *Nano Lett.* **2009**, *9*, 3676.

(6) (a) Costi, R; Saunders, A. E.; Banin, U. *Angew. Chem., Int. Ed.* **2010**, *49*, 4878. (b) Carbone, L.; Cozzoli, P. D. *Nano Today* **2011**, *5*, 449. (c) Li, X.; Lian, J.; Lin, M.; Chan, Y. *J. Am. Chem. Soc.* **2011**, *133*, 672.

(7) Amirav, L.; Alivisatos, A. P. *J. Phys. Chem. Lett.* **2010**, *1*, 1051.

(8) Habas, S. E.; Yang, P.; Mokari, T. *J. Am. Chem. Soc.* **2008**, *130*, 3294.

(9) (a) Dukovic, G.; Merkle, M. G.; Nelson, J. H.; Hughes, S. M.; Alivisatos, A. P. *Adv. Mater.* **2008**, *20*, 4306. (b) Alemseghed, M. G.; Ruberu, P. A.; Vela, J. *Chem. Mater.* **2011**, *23*, 3571.

(10) Elmalem, E.; Saunders, A. E.; Costi, R.; Salant, A.; Banin, U. *Adv. Mater.* **2008**, *20*, 4312.

(11) Talapin, D. V.; Nelson, J. H.; Shevchenko, E. V.; Aloni, S.; Sadtler, B.; Alivisatos, A. P. *Nano Lett.* **2007**, *7*, 2951.

(12) Fiore, A.; Mastria, R.; Lupo, M. G.; Lanzani, G.; Giannini, C.; Carlino, E.; Morello, G.; Giorgi, M. D.; Li, Y.; Cingolani, R.; Manna, L. *J. Am. Chem. Soc.* **2009**, *131*, 2274.

(13) Selvan, T.; Tan, T. T.; Ying, J. Y. *Adv. Mater.* **2005**, *17*, 1620.

(14) Wong, Y. J.; Zhu, L.; Teo, W. S.; Tan, Y. W.; Yang, Y.; Wang, C.; Chen, H. *J. Am. Chem. Soc.* **2011**, *133*, 11422.

(15) Viswanath, B.; Kundu, P.; Mukherjee, B.; Ravishankar, N. *Nanotechnology* **2008**, *19*, No. 195603.

(16) Salant, A.; Amitay-Sadovsky, E.; Banin, U. *J. Am. Chem. Soc.* **2006**, *128*, 10006.

(17) (a) Robinson, R. D.; Sadtler, B.; Demchenko, D. O.; Erdonmez, C. K.; Wang, L. W.; Alivisatos, A. P. *Science* **2007**, *317*, 355. (b) Jain, P. K.; Amirav, L.; Aloni, S.; Alivisatos, A. P. *J. Am. Chem. Soc.* **2010**, *132*, 9997. (c) Yin, Y. D.; Rioux, R. M.; Erdonmez, C. K.; Hughes, S.; Somorjai, G. A.; Alivisatos, A. P. *Science* **2004**, *304*, 711. (d) Sadtler, B.; Demchenko, D. O.; Zheng, H.; Hughes, S. M.; Merkle, M. G.; Dahmen, U.; Wang, L.-W.; Alivisatos, A. P. *J. Am. Chem. Soc.* **2009**, *131*, 5285.

(18) Yang, J.; Ying, J. Y. *Angew. Chem., Int. Ed.* **2011**, *50*, 4637.

(19) Mashkina, A. V.; Zirka, A. A. *Kinet. Catal.* **2000**, *41*, 521.

(20) Wark, S. E.; Hsia, C.-H.; Son, D. H. *J. Am. Chem. Soc.* **2008**, *130*, 9550.